Nuclear CK1δ as a Critical Determinant of PER:CRY Complex Dynamics and Circadian Period

Fidel E. Serrano[1], Daniela Marzoll[1], Bianca Ruppert[1], Axel C. R. Diernfellner[1], and Michael Brunner[1]*

[1]Heidelberg University Biochemistry Center, Im Neuenheimer Feld 328, D-69120 Heidelberg, Germany

*Corresponding author: michael.brunner@bzh.uni-heidelberg.de

Abstract

The mammalian circadian clock is governed by a feedback loop in which the transcription activator CLOCK:BMAL1 induces expression of its inhibitors, PERs and CRYs, which form a complex with CK1δ, the main circadian kinase. The spatiotemporal dynamics of this feedback mechanism and the precise role of CK1δ remain incompletely understood. Using an inducible cell system, we demonstrate that nuclear CK1δ is a key determinant of circadian period. The availability of CK1δ is limited due to rapid degradation and export of unassembled active kinase. Our findings reveal that active CK1δ promotes cytoplasmic localization of the PER2:CRY1 complex and triggers the dissociation of CRY1, which subsequently accumulates in the nucleus. We propose that late in the circadian cycle, cytoplasmic PER:CRY:CK1δ complexes may serve as a reservoir, gradually releasing CRY1 into the nucleus. This mechanism ensures rebinding of CLOCK:BMAL1 to DNA and prolonged attenuation of transcriptional activity after the degradation of PER proteins.

Keywords: Circadian clock, PERIOD, CRYPTOCHROME, Casein Kinase 1, nuclear-cytoplasmic shuttling

Introduction

Circadian clocks are molecular oscillators that regulate 24 h physiological rhythms as an adaptive response to day-night cycles[1,2]. In mammals, the core clock is based on a delayed negative transcription-translation feedback loop (TTFL), in which the transcriptional activators BMAL1 and CLOCK drive the expression of their inhibitors, PERIOD (PER) and CRYPTOCHROME (CRY) proteins[3–5]. This core loop is reinforced by a secondary feedback loop in which the nuclear receptors RORs and REV-ERBs connect the core oscillator to cellular metabolism by activating and repressing *BMAL1* transcription, respectively[6,7]. Circadian clocks are expressed in many tissues and entrained by recurring environmental cues. Entraining light cues are received by the suprachiasmatic nucleus (SCN), which directly and indirectly synchronizes clocks in peripheral organs via neuronal and hormonal/humoral cues. Recurring metabolic cues entrain peripheral clocks in the liver and other organs and determine their phase relative to the 24-hour light-dark cycle. The circadian system directly and indirectly controls key metabolic pathways[8–10].

The prevailing “dual-mode of circadian repression” model offers a robust framework for understanding the circadian clock on the molecular level, distinguishing between the so-called "early" and "late" repressive phases. During the early repressive phase, a complex composed of PERs, CRYs, and casein kinase 1δ (CK1δ) assembles on CLOCK:BMAL1, leading to CLOCK phosphorylation and displacement from DNA. In the late repressive phase, phosphorylated PER proteins undergo degradation, leaving CRY1 to directly suppress CLOCK:BMAL1 by sequestering the BMAL1 transactivation domain (TAD). Upon CLOCK dephosphorylation, the CLOCK:BMAL1 complex re-associates with DNA, establishing a poised promoter state. This configuration is

characterized by transcriptional readiness, awaiting CRY1 degradation to reinitiate the circadian transcriptional cycle[11–17].

Clock component homologs generally have redundant functions but differ in expression phases and binding affinities. PER1 and PER2 are crucial for robust clock function, with PER1 expressed earlier and shortening the circadian period, while PER2 lengthens period; PER3 plays a less critical role[18,19]. Similarly, CRY1 and CRY2, which differ in their affinity for CLOCK:BMAL1, have overlapping functions with CRY1 lengthening and CRY2 shortening circadian period[20]. The splice isoforms CK1δ1 and CK1δ2, and the similar CK1ε all support the clock, with their contributions varying potentially by tissue-specific expression[21,22]. Likewise, NPAS2 can partially substitute for CLOCK in a tissue-specific manner[23].

PER proteins serve as limiting scaffolds for the assembly of the repressive complex, playing a key role in circadian timing. CK1δ1 is crucial in regulating PER stability and function by phosphorylating PER proteins at numerous sites. A central aspect of this regulation involves the phosphorylation of serine 662 in human PER2 within the FASP (Familial Advanced Sleep Phase) region by CK1δ1 bound to the Casein Kinase Binding Domain (CKBD)[24,25]. This primes phosphorylation of four additional residues in the FASP region. When fully phosphorylated, the FASP region inhibits CK1δ1 by blocking its active site[26]. This attenuation slows the phosphorylation of serine 478, a residue within the β-TrCP phosphodegron, thereby delaying PER2 degradation, which is thus aligned with the circadian time frame[27]. This so-called "phosphoswitch" mechanism is well-characterized, involving the phosphorylation of five residues in the FASP region and one in the β-TrCP degron of PER2[27–29]. However, PER proteins are subjected to extensive hyperphosphorylation at numerous additional sites (about 80

in PER2) distributed across the protein[30]. While the kinetics of this widespread hyperphosphorylation strongly correlate with circadian timekeeping[31], the functional significance of these modifications remains largely unknown. It has been shown that phosphorylation of mPER1 masks an NLS[32]. The potential impact of PER phosphorylation on subcellular localization and interaction with other proteins has not been systematically analyzed. Furthermore, CK1δ is the main circadian kinase but has been implicated in other essential cellular functions including regulation of the cell cycle and Wnt signalling[33,34]. The regulation, subcellular distribution, and functional allocation of CK1δ to its various tasks have yet to be fully elucidated.

We utilized an inducible cellular overexpression system to investigate the dynamic interactions and subcellular localizations of CK1δ1, PER2, and CRY1. Our findings reveal that PER2 and CRY1 mutually influence their stability, as well as their nuclear-cytoplasmic shuttling dynamics and equilibrium. We demonstrate that CK1δ1 turnover and shuttling are regulated in a kinase activity-dependent manner such that free active CK1δ1 is rapidly degraded, making it a limiting factor for interactions with client proteins. Phosphorylation of PER2 by CK1δ1 drives its cytosolic localization and disrupts its interaction with CRY1, allowing CRY1 to translocate to the nucleus. Thus, cytoplasmic PER:CRY:CK1δ complexes may act as a buffer, with PER2 stabilizing and CK1δ1 slowly releasing CRY1 in a phosphorylation-dependent manner to sustain repression of CLOCK:BMAL1 during the late circadian phase.

Results

Overexpressed PER2 and CRY1 form dynamic nuclear foci

PER2 shuttles between nucleus and the cytosol and CRY1 facilitates nuclear localization of PER2[35–37]. To investigate the mechanism controlling the subcellular localization of PER2 and CRY1 alone and of both together, we tagged PER2 at its C-terminus with a mNeonGreen (mNG; PER2-mNG) moiety and CRY1 at its N-terminus with mKate2 (mK2; mK2-CRY1). Additionally, FLAG and 6xHis epitope tags were added to the PER2-mNG mK2-CRY1 constructs, respectively (Fig EV1A). The respective genes were expressed under control of a doxycycline (DOX)-inducible CMV promoter. U2OStx cells, which harbor a TET repressor (Life Technologies, R712-07), were transfected with PER2-mNG and mK2-CRY1. Expression was induced with DOX and after 24 h cells were analyzed by wide-field microscopy. The overexpressed proteins colocalized in nuclei and accumulated in foci (Fig 1A, B). We then generated a stable U2OStx cell line expressing PER2-mNG and mK2-CRY1. The cells expressed both proteins which colocalized in nuclear foci (Fig EV1B). Live-cell confocal microscopy revealed that the foci underwent fusion on the timescale of minutes (Fig EV1C), suggesting that overexpressed PER2-mNG and mK2-CRY1 formed phase-separated droplets. Since PERs and CRYs do not form thermodynamically stable, large detectable assemblies at native expression levels[38], a physiological function of their potential for self-interaction remains presently unclear.

To study the subcellular dynamics of the overexpressed clock proteins, U2OStx cells were transfected with PER2-mNG and mK2-CRY1 either separately or together at different ratios. Expression was induced with DOX and the dynamics of the subcellular localization and interaction (colocalization) of PER2-mNG and mK2-CRY1 was

analyzed at 4 h intervals over a time period of 28 h by live-cell microscopy using an Incucyte system (Fig 1C). Transient expression of mK2-CRY1 alone was observed after 4 h, with the protein localizing to the nucleus and remaining nuclear until it was degraded around 28 h post-DOX induction (Fig 1C, upper row). PER2-mNG by itself localized 4 h after DOX-induction predominantly in the cytosol and slowly relocalized to the nucleus over a time course of about 20 h (Fig 1C, bottom row). When PER2-mNG and mK2-CRY1 were coexpressed, the subcellular dynamics varied depending on their expression ratio. At a 1:3 transfection ratio of PER2-mNG : mK2-CRY1 (Fig 1C, 2nd row), mK2-CRY1 was nuclear at all times, and nuclear accumulation of PER2-mNG was accelerated, as previously reported[37]. At a 1:1 transfection ratio (Fig 1C, 3rd row), PER2-mNG accumulated in the nucleus more slowly, with some mK2-CRY1 colocalizing with PER2-mNG in the cytosol at early time points (4 h). At a 3:1 ratio (Fig 1C, 4th row), nuclear accumulation of PER2-mNG was slow and a substantial fraction of mK2-CRY1 localized with PER2-mNG in the cytosol for up to 16 h. The data indicate that PER2 and CRY1 mutually influence their nuclear-cytoplasmic shuttling dynamics and distribution.

To address why PER2-mNG alone changes its localization from initially cytosolic to eventually nuclear we inhibited CRM1-dependent nuclear export with leptomycin B (LMB). PER2-mNG then rapidly accumulated into the nucleus (Fig 1D), indicating that PER2-mNG was rapidly shuttling between cytosol and nucleus, in agreement with several previous reports[35,36]. Since nuclear-cytoplasmic shuttling of PER2-mNG was fast but it took many hours for PER2-mNG alone to accumulate in the nucleus, nuclear accumulation of the overexpressed PER2mNG likely depends on the slow synthesis of endogenous CRYs. Immunoblot analysis revealed that DOX-induced overexpression of PER2-mNG indeed supported expression of elevated levels of

endogenous CRY1 with kinetics similar to the nuclear accumulation of PER2-mNG (Fig 1E). Considering the low transfection efficiency of U2OStx cells with PER2-mNG, the accumulation of endogenous CRY1 in PER2-mNG transfected cells is substantial. Together, the data suggest that the ratio and hence degree of saturation of PER2-mNG, which is a dimer[39], with monomeric mK2-CRY1 determines their kinetics of nuclear import versus export.

PERs and CRYs in nuclear foci retain their interaction specificity

To functionally characterize the foci formed by the overexpressed clock proteins, a stable U2OStx_mK2-CRY1 line was transfected with untagged PER2 to induce formation of nuclear foci (Fig 2A). Since all cells express mK2-CRY1 and the transfection efficiency of U2OStx cells with PER2 was relatively low, the majority of cells displayed a homogenous nuclear distribution of mK2-CRY1 while fewer cells accumulated mK2-CRY1 in nuclear foci (Fig 2B and EV2A). Immunofluorescence (IF) with PER2 antibodies confirmed that overexpressed PER2 colocalized with mK2-CRY1 in nuclear foci while PER2 exhibited diffuse cellular localization in cells without foci. Further IF analyses revealed that endogenous PER1, BMAL1, and CK1δ1 colocalized in these nuclear foci (Figs 2C-E) in contrast to their dispersed subcellular distribution in cells that contained no foci (Fig EV2B-D). The data suggest that clock proteins are not recruited into pre-existing nuclear structures. Instead, PERs and CRYs have the capacity to form nuclear foci where they maintain specific interactions with other clock proteins. In the absence of these foci, CK1δ was distributed throughout the cell and concentrated in a single punctate structure (Fig EV2D), likely representing the centrosome, as previously reported[40]. Notably, CK1δ expression

levels were significantly elevated in cells containing nuclear PER2 and mK2-CRY1 foci, with the kinase also concentrated within these foci (Fig 2D). The data indicate that recruiting endogenous CK1δ into foci induced by overexpressed PER2 and mK2-CRY1 promotes the accumulation of elevated kinase levels.

CK1δ1 stability is regulated in an activity-dependent manner

To directly study the regulation of CK1δ1, we used previously generated stable U2OStx cell lines expressing the C-terminally FLAG-tagged wild-type CK1δ1 isoform, the tau-like mutant kinase CK1δ1-R178Q, and the kinase-dead version CK1δ1-K38R[31]. Upon DOX induction, mRNAs of the induced transgenes were expressed at similar levels, approximately 50-fold higher than the endogenous CK1δ RNA (Fig 3A). However, the proteins were expressed at vastly different levels (Fig 3B). CK1δ1 was expressed at the lowest level, CK1δ1-R178Q at an intermediate level, and CK1δ1-K38R at the highest level, suggesting an inverse correlation between resulting expression level and kinase activity. Immunoblot analysis using a CK1δ antibody revealed that, in the absence of DOX, FLAG-tagged kinases were leakily expressed at levels comparable to endogenous CK1δ (Fig 3B, bottom panel). Upon DOX induction, the FLAG-tagged kinases were overexpressed. We then tested whether the differences in resulting kinase expression were due to protein turnover. Following a cycloheximide (CHX) chase, overexpressed CK1δ1 was rapidly degraded with a half-time of less than 15 min, whereas CK1δ1-K38R and CK1δ1-R178Q remained stable (Fig 3C, E).

When U2OStx control cells were treated with CHX, endogenous CK1δ appeared to remained stable over the 90 min course (Fig 3D, E), consistent with previous

studies[3,41]. These data suggest that CK1δ is rapidly degraded only when overexpressed, likely due to a process facilitated by its enzymatic activity. In contrast, endogenous CK1δ, expressed at relatively lower physiological levels, may remain stable through interactions with various client proteins, which potentially protect it from degradation.

Since the mutant kinases CK1δ1-R178Q and CK1δ1-K38R were stable and expressed at higher levels than the more active CK1δ1, we investigated how pharmacological inhibition with PF670462 (hereafter referred to as PF670), a well-characterized inhibitor of CK1δ[42], affects the expression of both endogenous and overexpressed CK1δ1. Treatment with PF670 for 1 h stabilized overexpressed CK1δ1 but, consistent with previous reports, did not affect the abundance of endogenous CK1δ in U2OStx control cells (Fig 3F). Our data suggest that enzymatically active, overexpressed CK1δ1 is rapidly degraded, likely because it is not assembled with client proteins. CK1δ is a known target of the APC/C-Cdh1 ubiquitin ligase[43]. To further characterize the degradation pathway of CK1δ, we treated cells with the proteasome inhibitor MG132 (Fig 3G). In cells overexpressing CK1δ1, a 4 h treatment with MG132 led to a significant increase in CK1δ1 abundance, indicating that, in the absence of MG132, a large fraction of CK1δ1 synthesized from overexpressed RNA was degraded. CK1δ1-K38R was also stabilized by MG132 but to a lesser extent. In contrast, MG132 treatment of U2OStx control cells did not increase endogenous CK1δ levels within the 4 h time frame.

These findings suggest that the high levels of CK1δ1 produced from abundant DOX-induced mRNA are rapidly degraded in a kinase activity-dependent manner, presumably because the kinase is not assembled with client proteins. Due to the high synthesis rate of the overexpressed CK1δ1, a 1 h inhibition of kinase activity with

PF670 or a 4 h inhibition of protein turnover with MG132 was sufficient to raise CK1δ1 level to a detectable extent. In contrast, in control cells, the translation of endogenous CK1δ RNA (Fig 3A) was not sufficient to significantly increase kinase expression beyond the steady-state level within the inhibitor treatment time windows (Fig 3F, G). The data suggest that free CK1δ are present at low levels, potentially acting as a limiting factor for interactions with partners such as PER proteins.

PER2 supports accumulation of endogenous CK1δ

To investigate whether the expression of PER2, a known binding partner of CK1δ, is sufficient to elevate endogenous CK1δ levels, we generated stable U2OXtx cell lines that overexpress V5-tagged PER2 in a DOX-dependent manner. Upon induction of PER2 expression, endogenous CK1δ1 levels increased in parallel with PER2 requiring several hours for a detectable accumulation of the endogenous kinase (Fig 4A). CK1δ was hypophosphorylated, indicating that it was active and not undergoing autoinhibition[44]. The data suggest that PER2 acts as a stabilizing binding partner for newly synthesized CK1δ. A PER2-dependent increase in CK1δ1 expression was also observed when HEK293T cells were transfected with a constant amount of CK1δ1 plasmid along with increasing amounts of PER2 (Fig 4B). In contrast, the coexpression of PER2ΔCKBD, wherein the CK1 binding domain (CKBD) was deleted, did not lead to a substantial increase in CK1δ1 expression (Fig 4B). These findings suggest that the binding of CK1δ1 to the CKBD of PER2 plays a crucial role in protecting the kinase from degradation. The low level of CK1δ1 stabilization observed with PER2ΔCKBD may be attributed to the presence of an additional, albeit weak, CK1δ1 binding site in PER2ΔCKBD[45]. Alternatively, this stabilization could occur indirectly through the

PER2ΔCKBD-dependent stabilization of endogenous PERs, which could then provide a binding site for CK1δ1.

To analyze whether CRY1 affects the stabilization of CK1δ1 by PER2, we expressed the proteins in HEK293T cells (Fig 4C). When PER2 was expressed alone, it remained hypophosphorylated whereas CRY1 alone was expressed at a low level. However, coexpression with PER2 led to an elevated expression of CRY1, consistent with the role of PER2 in protecting CRY1 from proteasomal degradation by occupying the FBXL3 binding site[46,47]. Coexpression of CK1δ1 and CRY1 resulted in accumulation of low levels of both proteins. In contrast, when CK1δ1 was coexpressed with PER2, whether or not CRY1 was present, CK1δ1 accumulated at a high level. Since both CRY1 and CK1δ1 were tagged with a FLAG epitope, a comparison of their expression levels indicated that PER2 stabilized both proteins to a similar extent. Given that PER2 has a dedicated binding site for CRY1 and another for CK1δ1, this is consistent with a PER2 molecule stabilizing these proteins by binding a single molecule of each. The data suggest that, under conditions of overexpression, PER2 becomes saturated with CK1δ1 and CRY1, leading to its hyperphosphorylation, whereas at sub-saturating (i.e., endogenous) levels of CK1δ1 (Fig 4C, left lane), PER2 remains hypophosphorylated.

To investigate whether the stabilization of CK1δ1 was affected by kinase activity, we expressed the catalytically inactive CK1δ1-K38R and tau-like mutant kinase, CK1δ1-R178Q, which is less active than CK1δ1[31]. In the absence of V5-PER2, both mutant kinases were expressed at higher levels than CK1δ1, while CRY1 expression remained low (Fig EV3). Coexpression with PER2 further stabilized both mutant kinases, resulting in their accumulation at levels slightly higher than CK1δ1 (comp. Figs 4C and EV3 from the same blot). The data suggest that PER2 stabilizes CK1δ1

at a 1:1 ratio, while any excess kinase is degraded in a manner correlated with its kinase activity.

Active kinase is primarily degraded in the nucleus

We then analyzed the subcellular localization of CK1δ1 and how it was affected by kinase activity. Endogenous CK1δ1 exhibited a diffuse localization throughout U2OStx cells and a fraction of the kinase was concentrated at a punctate structure, presumably the centrosome as previously described[40,48,49] (Fig 5A, EV2d). Overexpressed CK1δ1 was highly enriched at the centrosome and displayed some enriched accumulation in the perinuclear region (Fig 5B, left panels). Kinase-dead CK1δ1-K38R was expressed at higher levels than CK1δ1, accumulated in the nucleus, in agreement with a previous report[50], and did not localize to the centrosome (Fig 5B, middle panels). Tau-like CK1δ1-R178Q was expressed at an intermediate level, somewhat enriched in the nucleus, and displayed centrosomal localization (Fig 5B, right panels). The elevated nuclear accumulation of tau-like kinase may, at least in part, explain the period-shortening phenotype observed in tau mutant animals[51,52]. These results suggest that the nuclear localization of CK1δ1 and its depletion from the centrosome is inversely related to its kinase activity. We confirmed this observation by treating U2OStx_CK1δ1 cells, and U2OStx cells for control, with either MG132 or PF670. Proteasomal inhibition with MG132 for 4 h led to an increase in overexpressed CK1δ1-FLAG throughout the cell and also at the centrosome (Fig 5C). The data demonstrate that centrosomal binding of CK1δ1 was not saturated, which may impact CK1δ1 availability for other binding partners, such as PERs. By contrast, CK1δ1-FLAG inhibited for 1 h with PF670 accumulated at elevated levels almost exclusively in the nucleus and its

centrosomal localization was lost (Fig 5D), as reported previously[48]. These findings suggest that the inhibition of kinase activity not only stabilizes overexpressed CK1δ1 but also promotes its accumulation in the nucleus and depletion from the cytosol and centrosome.

To determine whether kinase activity is directly required for centrosomal localization or rather for nuclear export, which might then indirectly promote centrosomal binding, we transiently transfected U2OStx cells with either CK1δ1-K38R-FLAG or CK1δ1-K38R-FLAG containing an N-terminal HIV-1 nuclear export signal (NES)[53]. While CK1δ1-K38R localized to the nucleus and was depleted from the centrosome, NES-CK1δ1-K38R was found in the cytosol and the centrosome (Fig 5E). These results demonstrate that CK1δ1 activity is essential for nuclear export but not for its localization to the centrosome per se. NES-CK1δ1-K38R was expressed at an ~5-fold higher level than CK1δ1-K38R (Fig 5E), indicating that inactive kinases, despite their increased stability, are preferentially degraded in the nucleus, potentially due to having more stabilizing binding partners in the cytosol. Treatment of U2OStx control cells with MG132 or PF670 resulted in a small, non-significant increase in levels of endogenous CK1δ1 (Fig EV4A, B). These data suggest that the physiological rate of kinase synthesis in U2OStx cells is rather low and insufficient to significantly increase CK1δ1 expression above steady state levels within the treatment windows of MG132 (4 h) and PF670 (1 h). Overall, these data indicate that overexpressed unassembled active CK1δ1 is highly unstable and preferentially degraded in the nucleus. The enzymatic activity of CK1δ1 facilitates its nuclear export and accelerates the nuclear degradation of unassembled CK1δ1, suggesting that CK1δ1 levels are generally low, with particularly low levels in the nucleus.

CK1δ1 facilitates cytoplasmic accumulation of PER2 and release of CRY1

To analyze whether CK1δ1 activity affects the localization and interaction of PER2 and CRY1, we transfected U2OStx_CK1δ1 and U2OStx_CK1δ1-K38R cells with PER2-mNG and mK2-CRY1. Expression and localization of the DOX-induced proteins was analyzed by live cell microscopy over a time course of 28 h. In U2OStx_CK1δ1-K38R, PER2-mNG alone accumulated initially in the cytosol and relocated slowly to the nucleus (Fig EV5A, upper panels), similar to what was observed in absence of kinase (see Fig 1C, lower panels). However, in U2OStx_CK1δ1 cells, PER2-mNG remained cytosolic (Fig EV5A lower panels). Considering that PER2-mNG shuttles rapidly between nucleus and cytosol (see Fig 1d), the data suggest that coexpression of active kinase results in cytoplasmic localization of PER2, likely via a previously reported mechanism of inactivation of an NLS[32].

Upon coexpression of PER2-mNG and mK2-CRY1 in U2OStx_CK1δ1-K38R, the proteins accumulated in the nucleus and formed foci, which persisted for 28 h and longer (Fig 6A, upper panels), similar to what was observed in absence of overexpressed kinase (see Fig 1C, middle panels). The data indicate that the catalytically inactive CK1δ1-K38R did not affect the expression and localization of PER2-mNG and mK2-CRY1. In contrast, in U2OStx_CK1δ1 cells, PER2-mNG and mK2-CRY1 accumulated in cytosolic foci with a substantial fraction of mK2-CRY1 accumulating in the nucleus without PER2-mNG (Fig 6A, lower panels and EV5B). The foci grew in size up to about 16 h post DOX-induction and after about 20 h, PER2-mNG was degraded. mK2-CRY1 was then exclusively detected in the nucleus and levels decreased over time with substantially slower kinetics than cytoplasmic mK2-CRY1 and PER2-mNG. This suggests that free nuclear mK2-CRY1 represents a pool that either migrates to the nucleus upon phosphorylation-dependent PER2-mNG

degradation and/or is released from PER2-mNG, potentially regulated by phosphorylation.

We then quantified the relative ratio of mK2-CRY1 to PER2-mNG in cytosolic versus nuclear foci. This analysis revealed that the cytoplasmic PER:CRY foci in cells expressing active CK1δ1 contained one third less mK2-CRY1 compared to the nuclear PER:CRY foci in cells expressing the inactive CK1δ1-K38R (Fig 6B), suggesting that CK1δ1 is also released from cytoplasmic foci prior to degradation of PER2-mNG.

To investigate whether CK1δ1-mediated phosphorylation triggers the release of CRY1 from PER2, we prepared a native cell extract from HEK293T cells overexpressing V5-PER2 and CRY1-FLAG which was then incubated with purified CK1δΔtail in an *in vitro* phosphorylation reaction[31]. In the presence of kinase, PER2 was hyperphosphorylated while the electrophoretic mobility of CRY1 did not shift (Fig 6C). Subsequent immunoprecipitation revealed that CRY1 co-immunoprecipitated with unphosphorylated but not with hyperphosphorylated V5-PER2 (Fig 6C). The data suggest that CK1δ1-mediated phosphorylation of PER2 promotes the release of bound CRY1. To explore this further, we transfected stable U2OStx_mK2-CRY1 cells with PER2-mNG and untagged CK1δ1, and induced expression with DOX (Fig 6d and EV5C). The majority of cells expressed only mK2-CRY1, indicating that they remained untransfected. In contrast, cells exhibiting cytoplasmic foci of PER2-mNG were identified as cotransfected with untagged CK1δ1, as the foci become cytoplasmic only under these conditions. Tracking the DOX-induced protein dynamics over a 28-hour time course, we observed that mK2-CRY1 was depleted in untransfected cells, likely due to metabolism of DOX[54]. Interestingly, in transfected cells, mK2-CRY1 initially colocalized with PER2-mNG in cytoplasmic foci. Upon PER2-mNG degradation, liberated mK2-CRY1 translocated and accumulated at elevated levels in the nucleus.

This led to sustained nuclear levels of mK2-CRY1 in cells initially expressing PER2-mNG and CK1δ1, even at later time points when mK2-CRY1 had already been depleted in neighbouring untransfected cells. Thus, cytoplasmic PER2 and the resulting cytoplasmic PER:CRY complexes may act as a reservoir, progressively releasing CRY1 into the nucleus in a CK1δ1-dependent manner, a process that is formally analogous to the *de novo* synthesis of CRY1 from its mRNA. The phosphorylation-dependent cytoplasmic localization of PER2-mNG and the slow release of mK2-CRY1 effectively decouples CRY1 subcellular localization, repressive activity, and degradation from those of PER2. It has been shown that nuclear CRY1 forms a repressive complex with CLOCK:BMAL1 late in the circadian cycle[14,41]. Since CRY1 is rapidly degraded on its own, our findings suggest that the CK1δ1-dependent release of CRY1 from cytoplasmic PER2 may play a crucial role in maintaining sufficient nuclear CRY1 levels for repression during the late circadian phase.

Nuclear CK1δ1 affects circadian period length

Our data show that overexpressed and unassembled CK1δ1 is rapidly degraded via the proteasome. The fact that MG132 treatment for 4 h did not increase the levels of endogenous CK1δ1 in U2OStx cells suggests that its synthesis rate is relatively low (Fig 3G). Hence, in a circadian cycle, the accumulation of PER2 might initially exceed the amount of CK1δ1 freely available for assembly into the PER:CRY complex, potentially causing PERs together with CRYs to enter the nucleus without CK1δ1 and only later assemble with CK1δ1 within the nucleus. To analyze whether PER2 recruits CK1δ1 preferentially in the cytosol or the nucleus, we constructed CK1δ1-FLAG fusion proteins with an N-terminal mNeonGreen tag followed by either an SV40 nuclear

localization signal (NLS)[55] or an HIV-1 nuclear export signal (NES)[53] (Fig 7A). To characterize the subcellular localization and stability of the kinases, U2OStx cells were transiently transfected with these mNG-CK1δ1 constructs. Next day, the expression was induced with DOX for 24 h, and cells were then treated with or without MG132 for 4 h. mNG-NLS-CK1δ1 was expressed at a low level and localized to the nucleus (Fig 7b, left panel), while mNG-NES-CK1δ1 accumulated in the cytosol (Fig 7b, right panel), demonstrating that the added localization signals determined the subcellular localization of the kinases. MG132 treatment stabilized mNG-NLS-CK1δ1-FLAG about 8-fold (Fig 7B), while mNG-NES- CK1δ1-FLAG was stabilized only about 1.8-fold (Fig 7C). The data indicate that, in the absence of MG132, overexpressed mNG-NLS-CK1δ1 is rapidly degraded by the nuclear proteasome, while overexpressed mNG-NES-CK1δ1 escapes efficient nuclear degradation by export into the cytosol, where it is turned over at a lower rate. To assess how the cytoplasmic and nuclear kinases affect the circadian clock we generated and selected stable U2OStx cell lines expressing in DOX-inducible manner similar levels of mNG-NLS-CK1δ1 and mNG-NES-CK1δ1, respectively (Fig 7D). To monitor the circadian rhythm, cells were transfected with a *Bmal1* promoter (Bmal1p)-luc reporter. Cells were then incubated with or without DOX and Bmal1p-luc expression was recorded for 96 h. Expression of mNG-NLS-CK1δ1 shortened the circadian period by 4 h (Fig 7E, upper panel and F), while mNG-NES-CK1δ1-FLAG had no impact on period length (Fig 7E, lower panel and F). The data suggest that cytoplasmic mNG-NES-CK1δ1 does not interfere with the function of endogenous PERs, likely because PER:CRY complexes are rapidly imported and retained in the nucleus, where they gradually assemble with the low levels of endogenous CK1δ1 to sustain the circadian clock. When sufficient CK1δ1 is assembled into the nuclear PER:CRY complex, PER phosphorylation results in the

export of the resulting PER:CRY:CK1δ1 complex into the cytoplasm. Integrating this with our previous observations, this now cytoplasmic PER:CRY:CK1δ1 complex can serve as a buffer to release CRY1 into the nucleus to sustain a prolonged late repressive phase.

Discussion

The dual-mode circadian repression model describes three distinct phases of CLOCK:BMAL1 activity, regulated in temporal succession by CRY1/2, PER1/2, and CK1δ/ε[12–17]. Initially, CLOCK:BMAL1 is repressed via PER:CRY:CK1δ-mediated displacement, followed by CRY1-dependent blocking of DNA-bound CLOCK:BMAL1, and finally derepression of CLOCK:BMAL1 when PER and CRY proteins are degraded. In this model, CK1δ/ε is assumed to be non-limiting and readily available to PER proteins as they are synthesized in the cytosol.

The data presented here suggest that freely available CK1δ is limited, as unassembled kinase is rapidly degraded. We demonstrate that free active CK1δ is especially scarce in the nucleus due to both rapid degradation and activity-dependent export to the cytosol. Notably, increasing specifically nuclear CK1δ through targeted overexpression shortens the circadian period, indicating that nuclear CK1δ levels serve as a period-limiting factor.

Since PER:CRY:CK1δ complexes phosphorylate CLOCK[14], CK1δ-dependent enzymatic inhibition of CLOCK:BMAL1 may operate effectively even at substoichiometric concentrations. In contrast, CRY1-mediated non-catalytic, sequestration-type repression likely requires near-saturating CRY1 levels to sequester a significant fraction of BMAL1's transcriptional activation domain (TAD). Thus, the limited availability of CK1δ for newly synthesized PER proteins may delay phosphorylation-dependent repression, providing time for sufficient PER:CRY complex accumulation to ensure robust CRY-dependent repression later in the circadian cycle.

Since CK1δ1 degradation and nuclear export depend on its kinase activity, we observed that the less active tau-like CK1δ1-R178Q mutant accumulates at elevated nuclear levels. According to the phosphoswitch model, the tau mutation (e.g., R178C in CK1δ) shortens the circadian period by slowing phosphorylation of the FASP region in PER2, which in turn facilitates faster phosphorylation of the β-TrCP degron site (S478 in mPER2). We demonstrate that the period shortening induced by the tau-like CK1δ1-R178Q mutant[31] can be replicated by forcing nuclear accumulation of wild-type CK1δ1 using an NLS tag (mNG-NLS-CK1δ1). These findings suggest that the period-shortening effect of tau mutations may in part stem from increased nuclear levels of the less active tau-mutant CK1δ/ε.

This study further explores the relationship between PER:CRY:CK1δ complexes and CRY1. The current circadian model suggests that the cycle is regulated by the rhythmic abundance of PER:CRY:CK1δ complexes, with late-phase repression by CRY1 alone persisting for several hours after CK1δ-dependent degradation of PER proteins. Our findings suggest that CK1δ-mediated phosphorylation not only facilitates PER2 degradation but also promotes its cytosolic accumulation and triggers the dissociation of bound CRY1. Incorporating these results into the circadian framework implies that, late in the cycle, nuclear PER2:CRY1:CK1δ levels decline due to both degradation and cytoplasmic localization. Reduction of nuclear PER2:CRY1:CK1δ levels below a critical threshold is necessary for dephosphorylation of CLOCK and rebinding of CLOCK:BMAL1 to DNA. Cytosolic PER2:CRY1:CK1δ complexes may then serve as a reservoir, gradually releasing CRY1 in a CK1δ-dependent manner to support repression of DNA-bound CLOCK:BMAL1. Endogenous as well as endogenously tagged PER2 have been detected in the cytosol during the late repressive phase[36,56]. Our data show that nuclear CRY1 levels are indeed much higher

and persist for a longer time in stable CRY1-expressing cells that accumulate PER2 and CK1δ1 in the cytosol.

Both PER2:CRY1/2:CK1δ complexes and CRY1 alone have the potential to repress CLOCK:BMAL1, prompting the question of why the mammalian circadian clock utilizes both modes of repression. Published data suggest that CRY1 is present and plays a role throughout the entire circadian cycle: While both PER and CRY proteins are rhythmically expressed, quantitative analyses show that PER protein levels are very low when CLOCK:BMAL1 activity reaches its circadian maximum, whereas CRY1 remains at about 50% of its peak level[57]. Furthermore, ChIP-seq data from mouse liver reveal that CRY1 is present at circadian promoters not only during the late repressive phase (CT0-4) but also substantially at CT8-12, when CLOCK:BMAL1 activity is maximal[11]. Finally, in CRY1 knock-out U2OS cells, endogenously tagged P*ER2-LUC* oscillated at elevated levels[58], suggesting that in wild-type cells, CRY1 partially represses CLOCK:BMAL1 even when circadian transcription is at its peak. These findings suggest that CRY1 attenuates CLOCK:BMAL1 activity throughout the circadian cycle.

The interaction of CRY1 with DNA-bound CLOCK:BMAL1 establishes a poised promoter state, characterized by early transcription termination and the cycling of initiating Pol II[11]. The release of paused/cycling Pol II into productive transcription elongation represents a critical regulatory step in transcription. Establishing this poised state at CLOCK:BMAL1 target promoters may not only ensure efficient repression during the late repressive phase, when CRY1 levels are high, but may also modulate the extent of promoter activation later in the cycle according to the residual CRY1

levels. The release of CRY1 from cytoplasmic PER:CRY complexes may contribute to this regulation.

Consequently, while PER2:CRY1/2:CK1δ complexes regulate the troughs of circadian gene expression, CRY1 may limit the circadian peak levels of CLOCK:BMAL1-dependent transcription.

In summary, many of our conclusions are based on the combination of transient transfection, synchronized DOX-induced expression of tagged clock proteins, and Incucyte live-cell microscopy, which enabled observations that were otherwise challenging. Yet, this approach has obvious limitations. Firstly, it is restricted to only two fluorescent colors, necessitating the inference of a third unlabeled protein's expression based on the phenotypes of the two tagged proteins. Additionally, the expression ratios of transfected proteins vary among individual cells, and DOX-induced expression is not constant over time, even for stably integrated genes. Furthermore, overexpression of PER2 and CRY1 induces the formation of foci, presumably phase-separated droplets, while the endogenous proteins do not accumulate in thermodynamically persisting assemblies of detectable size. These factors complicate the analysis and interpretation of temporal and spatial dynamics.

Yet, our data provide strong evidence that early in the circadian cycle CK1δ is not readily available for PER proteins allowing nuclear accumulation of PER:CRY complexes. Late in the circadian cycle phosphorylation of PER2 by CK1δ promotes its accumulation in the cytosol and facilitates the release of CRY1 prior to PER2 degradation (Fig EV6).

Methods

Plasmids

For cloning using restriction enzymes. Enzymes used for cloning were obtained from New England Biolabs (NEB). Restriction digestion, dephosphorylation of vector backbone and ligation was performed as recommended by NEB. Linear DNA was purified using NucleoSpin Gel and PCR Clean-up kit from Macherey-Nagel. Plasmids were extracted with GeneJET Plasmid Miniprep kit from Thermo Fisher Scientific. For cloning with overlapping regions (restriction enzyme-free cloning), enzymes (Q5 DNA polymerase, restriction enzyme DpnI and T4 DNA polymerase) were obtained from NEB. DpnI digestion and exonuclease reaction with T4 DNA polymerase was performed in NEBuffer 2.1. *E. coli* were transformed with exonuclease treated PCR product(s) to facilitate *in vivo* plasmid assembly via overlapping DNA ends. pcDNA4/TO-derived vectors were constructed by cloning the coding regions of human casein kinase 1 isoform delta (CK1δ), murine Period circadian protein homolog 2 (mPer2), and murine cryptochrome 1 (mCry1) downstream of the CMV-TetO2 promoter which allows for DOX-inducible protein expression in cells harboring the tetracycline-repressor cassette (tx; i.e., U2OStx) and constitutively high expression in cells without the tetracycline-repressor cassette (i.e., HEK293T). Mutations, fluorescent tags, and epitopes were introduced by via ligation-free overlap cloning. All plasmid DNA sequences were sequence-verified prior to use.

Cell lines

T-REx-U2OS (U2OStx; Life Technologies) and HEK293T (ATCC) cells were maintained in Dulbecco's Modified Eagle Medium (DMEM) supplemented with 10% Fetal Bovine Serum (FBS) and 1x Penicillin-Streptomycin (Pen-strep). Cell culture

reagents were obtained from Life Technologies. Cells were grown and maintained at 37°C in a humidified incubator containing 5% CO2.

For plasmid transfection, U2OStx cells were transfected with Xfect Transfection Reagent (Takaka) following the manufacturer's protocol whereas HEK293T cells were transfected with polyethylenimine (PEI, made in-house) following the conventional protocol. To generate stable U2OStx cell lines, basal U2OStx cells were seeded in a 24-well plate and grown to confluence overnight. Cells were transfected with pcDNA4/TO vectors containing the desired constructs. Stable transfectants were selected by growing cells to sub-confluence in complete media supplemented with 50 µg/mL hygromycin and 100 µg/mL zeocin (Invitrogen) over the course of two to three weeks. Resulting single cell colonies after selection were isolated for further experimentation as previously described. To induce protein overexpression, cells were treated with 10 ng/mL DOX.

Immunofluorescence

Cells were seeded on 12mm #1.0 glass coverslips (VWR, CAT# 631-1577P) in 500 µL media. Whenever applicable, transient transfection and/or DOX induction was performed. Immunofluorescence was done 24 h post-induction. Cells were washed with PBS and fixed with 4% paraformaldehyde for 10 min at room temperature. Cells were permeabilized with PBS + 0.1% Triton X-100 for 10 min, then washed three times and blocked with PBS + 5% heat-inactivated FBS for 1 h. Cells were then treated with the following primary antibodies diluted in PBS + 3% BSA + 0.25% Tween20 for 1 h at 37°C: PER2 (in-house, 1:50, rabbit polyclonal), PER1 (in-house, 1:100, rabbit polyclonal), BMAL1 (in-house, 1:200, rabbit polyclonal)[59,60], CK1δ (Abcam ab85320, 1:1000), FLAG (Sigma-Aldrich F3165, 1:200). This was followed by washing with PBS,

and treatment with corresponding secondary antibody: goat anti-rabbit conjugated to AlexaFluor488 (Thermo Fisher Scientific A-11008, 1:500) or goat anti-mouse conjugated to AlexaFluor488 (Thermo Fisher Scientific A-11001, 1:500) diluted in PBS + 3% BSA + 0.25% Tween20 for 1 h at 37°C. Cells were again washed three times, then mounted onto glass slides with ProLong™ Glass Antifade Mountant with NucBlue (Thermo Fisher Scientific P36983) and sealed with nail polish.

Fluorescence, time-lapse, and live-cell confocal microscopy

For microscopy of fluorescently-tagged proteins and immunofluorescence, a Nikon Ni-E microscope was used (Nikon Imaging Center, Heidelberg) at a 60X oil immersion objective and the corresponding filter sets for DAPI, FITC, and Cy5. Exposure times were optimized within each experiment to obtain comparable fluorescence intensities. For image acquisition, the central focal plane was determined and images were taken as at 0.3 µm z-steps to a total 11 steps. For time-lapse microscopy, an Incucyte S3 system (Sartorius) was used at a 20X objective using the built-in filter sets set for the green and red channel. Exposure times were optimized within each experiment to obtain comparable fluorescence intensities. Images were taken at a regular schedule every 4 h until the end of the experiment typically 48 h later. For time-lapse, live-cell, confocal microscopy, a Nikon A1R confocal microscope was used (Nikon Imaging Center, Heidelberg) with a built-in TokaiHit on-stage environmental chamber. To prevent autofluorescence, colorless DMEM supplemented with normocin was used. Additionally, 60X oil immersion objective and the corresponding laser and filter sets for DAPI, FITC, TRITC, and TD (brightfield) were used. Exposure times were optimized within each experiment to obtain comparable fluorescence intensities. For image acquisition, the central focal plane was determined and images were taken as

at 1.5 µm z-steps to a total 5 steps. Images were taken every 5 min for 17 h. All resulting images were exported and digital image analysis was performed in FIJI.

Quantitative PCR

Cells were grown in p24 plates and induced with DOX for 24 h. RNA was extracted using peqGOLD TriFast Reagent following manufacturer's protocols. cDNA was reverse-transcribed from 500 ng total RNA extract with Maxima Reverse Transcriptase (Thermo Fisher Scientific) following manufacturer's protocols. Quantitative PCR (qPCR) was performed on a StepOne™ Real-Time PCR System (Applied Biosystems, Themo Fisher Scientific, CAT# 4376598) using Maxima SYBR Green qPCR Master Mix (Thermo Fisher Scientific) following manufacturer's protocols. The following primer pairs below were used for their respective targets: CK1-F: AACCAAACACCCTCAGCTCCAC and CK1-R: GCCCCAGCAGCTCCATCACCAT; GAPDH-F: TGCACCACCAACTGCTTAGC and GAPDH-R: ACAGTCTTCTGGGTGGCAGTG. Relative gene expression was normalized to GAPDH and calculated using the $\Delta\Delta C_T$ method. Further normalization to the DOX-induced U2OStx sample was done to determine fold induction of gene expression.

Immunoblotting

Protein extraction was performed using an in-house lysis buffer (25 mM Tris-HCl, pH 8.0, 150 mM NaCl, 0.5% Triton X100, 2 mM EDTA, 1 mM NaF, freshly added protease inhibitors: 1 mM phenylmethylsulfonyl fluoride (PMSF), leupeptin (5 µg/ml), and pepstatin A (5 µg/ml)) according to the conventional protocol. Briefly, cells were scraped and sample was collected via centrifugation. The sample was incubated in ice-cold lysis buffer on ice for 10 min and then incubated in a sonicated water bath for 10 min. Samples were centrifuged at 16,000 x g, 4 °C, 15 min taking the supernatant.

Protein concentration was quantified via Nanodrop (NP80, Implen). For immunoblot analysis, protein samples were analzyed by SDS-polyacrylamide gel electrophoresis and transferred to a nitrocellulose membrane (cytiva, Amersham Protran, 0.45 µm pore size) via semi-dry blotting. To control for protein loading, membranes were stained with Ponceau S. Membranes were typically incubated in primary antibody at 4°C overnight and in secondary antibody conjugated to horseradish peroxidase at room temperature for 2 h. The following primary antibodies were used: anti-FLAG (Sigma-Aldrich F3165, 1:5000, mouse monoclonal), anti-CK1δ (abcam AF12G4, 1:5000, mouse monoclonal), anti-V5 (Invitrogen R960-25, 1:5000, mouse monoclonal); and the following secondary antibody was used for luminescent detection: goat anti-mouse IgG (H+L)-HRP conjugate (Bio-Rad 170-6516, 1:10000). For decoration, membranes were incubated in decoration buffer (100 mM TrisHCl pH 8.5, 2.2 x 10-2 % (w/v) luminol, 3.3 x 10-3 % (w/v) coumaric acid, 9.0 x 10-3 % (v/v) H2O2) and exposed for a time series to X-ray films (Fujifilm). Films were then developed (Medical film processor from Konica Minolta). Densitometric analysis of immunoblots was done using the built-in module in FIJI. The results were measured and plotted onto GraphPad Prism for downstream analysis (i.e., plotting over time post-CHX chase).

Cycloheximide chase; MG132, PF670 Treatments

Unless otherwise stated, induction of protein expression was typically performed by addition of 10 ng/mL doxycycline (DOX; Thermo Fisher Scientific CAT# 631311) 24 h prior to downstream experiments. To arrest protein translation for a cycloheximide (CHX) chase, CHX was added to our cells to a final concentration of 10 µg/ml. Untreated samples were taken as the 0 min CHX sample. Samples were then taken at 15, 30, 45, 60, and 90 min post-CHX for protein extraction and immunoblotting. To

inhibit the proteosome, cells were treated with 20 µM MG132 (Abmole Bioscience CAT# AMO-M1902) for 4 h prior to immunoblotting; 4 µM MG132 for 4 h prior to immunofluorescence. To inhibit CK1δ; cells were treated with 1 µM PF670462 (Tocris Biosciences CAT# 3316) for 4 h prior to immunoblotting and immunofluorescence. To inhibit phosphatases, cells were treated with 80 nM CalA (LC Labs Cat# C-3987) for 60, 20, 6, and 0 (untreated) min. All chemical treatments were performed with the corresponding solvent (vehicle) control: DMSO for MG132, and H2O for PF670.

in vitro phosphorylation assay and co-immunoprecipitation

HEK293T cells were transfected with V5-PER2 and CRY1-FLAG and the lysate was used as a starting material for an *in vitro* phosphorylation assay. CK1δΔtail was purified and used as the kinase for an *in vitro* phosphorylation assay as previously described[31]. As a negative control, a reaction mix containing all of the reaction buffer components except for the $MgCl_2$ was incubated with the sample in the absence of additional kinase. The in vitro phosphorylation reaction was carried out at 4°C for 6 h. The reaction was stopped using PF670 prior to subsequent co-IP. For co-IP, Protein G Sepharose 4 Fast Flow (cytiva, 17061802) beads were used following the manufacturer's protocol. Briefly, a 1:1 slurry was prepared by repetitive washing and buffer exchange with 67% TBS. The beads were then incubated with anti-V5 antibody (Thermo Fisher Scientific, R960) at 4°C while rotating for 4 h and used directly. Resulting samples following an *in vitro* phosphorylation assay were loaded onto the beads and incubated at 4°C overnight. Supernatant was removed, and the beads were then washed thrice with cold 67% TBS and gently centrifuged at 300 x g, 4°C, for 30 s. Bound protein was eluted using 2x Laemmli buffer without β-mercaptoethanol and boiling at 95°C for 5 min. Corresponding "Input" and "IP" samples were taken and

loaded onto a PAGE gel. For the IP sample, an 8x equivalent was loaded compared to Input.

Luciferase reporter assay

Bioluminescence of luciferase reporter genes was performed as previously described[31]. Briefly, samples were measured with a plate reader (EnSpire from PerkinElmer) placed in a temperature-controlled incubator (CLF Plant Climatics E41L1C8). Cells were seeded in a white 96-well plate and transfected using Xfect with Bmal1p-luc vector[61]. Cells were synchronized via medium change using media supplemented with either PBS or DOX. The plate was sealed and bioluminescence was recorded at 30 min intervals at 37°C. Three independent experiments with four technical replicates per cell line and treatment were carried out. Resulting bioluminescence traces were detrended using a sliding 24h-time window for baseline subtraction and a sliding 3h-time window for smoothening. Circadian period was determined using the curve-fitting function to a non-linear damped sine wave function in GraphPad Prism 10.

Statistical Analysis

Data were plotted on GraphPad Prism 10. To test for differences between two samples, student's t-test was performed. To test for difference between three or more samples, ANOVA was performed. Statistical significance was defined by a p value of < 0.05. All data are presented as means ± standard deviations (SD).

Acknowledgements

We thank Alessia Ruggieri und Michael Knop for providing mKATE-2 and mNeonGreen templates, respectively. This work was supported by the Deutsche Forschungsgemeinschaft, TRR186.

Ethics declarations

Competing interests

The authors declare no competing interests.

Data Availability

The data supporting the findings of this study are available within the article and its supplementary information files. This study includes no data deposited in external repositories.

Material Availability

Plasmids and cell lines generated in this study are available from the lead contact, Michael Brunner (michael.brunner@bzh.uni-heidelberg.de) with a completed materials transfer agreement.

References

1. Takahashi, J. S. Transcriptional architecture of the mammalian circadian clock. *Nat Rev Genet* **18**, 164–179 (2017).
2. Partch, C. L. Orchestration of Circadian Timing by Macromolecular Protein Assemblies. *Journal of Molecular Biology* **432**, 3426–3448 (2020).
3. Lee, C., Etchegaray, J.-P., Cagampang, F. R. A., Loudon, A. S. I. & Reppert, S. M. Posttranslational Mechanisms Regulate the Mammalian Circadian Clock. *Cell* **107**, 855–867 (2001).
4. Bell-Pedersen, D. *et al.* Circadian rhythms from multiple oscillators: lessons from diverse organisms. *Nat Rev Genet* **6**, 544–556 (2005).
5. Partch, C. L., Green, C. B. & Takahashi, J. S. Molecular architecture of the mammalian circadian clock. *Trends in Cell Biology* **24**, 90–99 (2014).
6. Preitner, N. *et al.* The Orphan Nuclear Receptor REV-ERBα Controls Circadian Transcription within the Positive Limb of the Mammalian Circadian Oscillator. *Cell* **110**, 251–260 (2002).
7. Sato, T. K. *et al.* A Functional Genomics Strategy Reveals Rora as a Component of the Mammalian Circadian Clock. *Neuron* **43**, 527–537 (2004).
8. Moynihan Ramsey, K., Marcheva, B., Kohsaka, A. & Bass, J. The Clockwork of Metabolism. *Annu. Rev. Nutr.* **27**, 219–240 (2007).
9. Dibner, C., Schibler, U. & Albrecht, U. The Mammalian Circadian Timing System: Organization and Coordination of Central and Peripheral Clocks. *Annu. Rev. Physiol.* **72**, 517–549 (2010).
10. Mohawk, J. A., Green, C. B. & Takahashi, J. S. Central and Peripheral Circadian Clocks in Mammals. *Annu. Rev. Neurosci.* **35**, 445–462 (2012).

11. Koike, N. *et al.* Transcriptional Architecture and Chromatin Landscape of the Core Circadian Clock in Mammals. *Science* **338**, 349–354 (2012).
12. Ye, R. *et al.* Dual modes of CLOCK:BMAL1 inhibition mediated by Cryptochrome and Period proteins in the mammalian circadian clock. *Genes Dev* **28**, 1989–1998 (2014).
13. Chiou, Y.-Y. *et al.* Mammalian Period represses and de-represses transcription by displacing CLOCK–BMAL1 from promoters in a Cryptochrome-dependent manner. *Proc. Natl. Acad. Sci. U.S.A.* **113**, (2016).
14. Aryal, R. P. *et al.* Macromolecular Assemblies of the Mammalian Circadian Clock. *Molecular Cell* **67**, 770-782.e6 (2017).
15. Michael, A. K. *et al.* Formation of a repressive complex in the mammalian circadian clock is mediated by the secondary pocket of CRY1. *Proc. Natl. Acad. Sci. U.S.A.* **114**, 1560–1565 (2017).
16. Fribourgh, J. L. *et al.* Dynamics at the serine loop underlie differential affinity of cryptochromes for CLOCK:BMAL1 to control circadian timing. *eLife* **9**, e55275 (2020).
17. Cao, X., Yang, Y., Selby, C. P., Liu, Z. & Sancar, A. Molecular mechanism of the repressive phase of the mammalian circadian clock. *Proc. Natl. Acad. Sci. U.S.A.* **118**, e2021174118 (2021).
18. Bae, K. *et al.* Differential Functions of mPer1, mPer2, and mPer3 in the SCN Circadian Clock. *Neuron* **30**, 525–536 (2001).
19. Zheng, B. *et al.* Nonredundant Roles of the mPer1 and mPer2 Genes in the Mammalian Circadian Clock. *Cell* **105**, 683–694 (2001).
20. Horst, G. T. J. V. D. *et al.* Mammalian Cry1 and Cry2 are essential for maintenance of circadian rhythms. *Nature* **398**, 627–630 (1999).

21. Fustin, J.-M. *et al.* Two *Ck1δ* transcripts regulated by m6A methylation code for two antagonistic kinases in the control of the circadian clock. *Proc. Natl. Acad. Sci. U.S.A.* **115**, 5980–5985 (2018).
22. Lee, H., Chen, R., Lee, Y., Yoo, S. & Lee, C. Essential roles of CKIδ and CKIε in the mammalian circadian clock. *Proc. Natl. Acad. Sci. U.S.A.* **106**, 21359–21364 (2009).
23. Landgraf, D., Wang, L. L., Diemer, T. & Welsh, D. K. NPAS2 Compensates for Loss of CLOCK in Peripheral Circadian Oscillators. *PLoS Genet* **12**, e1005882 (2016).
24. Toh, K. L. *et al.* An hPer2 Phosphorylation Site Mutation in Familial Advanced Sleep Phase Syndrome. *Science* **291**, 1040–1043 (2001).
25. Vanselow, K. *et al.* Differential effects of PER2 phosphorylation: molecular basis for the human familial advanced sleep phase syndrome (FASPS). *Genes Dev.* **20**, 2660–2672 (2006).
26. Philpott, J. M. *et al.* PERIOD phosphorylation leads to feedback inhibition of CK1 activity to control circadian period. *Molecular Cell* **83**, 1677-1692.e8 (2023).
27. Zhou, M., Kim, J. K., Eng, G. W. L., Forger, D. B. & Virshup, D. M. A Period2 Phosphoswitch Regulates and Temperature Compensates Circadian Period. *Molecular Cell* **60**, 77–88 (2015).
28. Philpott, J. M. *et al.* Casein kinase 1 dynamics underlie substrate selectivity and the PER2 circadian phosphoswitch. *eLife* **9**, e52343 (2020).
29. Narasimamurthy, R. *et al.* CK1δ/ε protein kinase primes the PER2 circadian phosphoswitch. *Proc. Natl. Acad. Sci. U.S.A.* **115**, 5986–5991 (2018).
30. Hornbeck, P. V. *et al.* PhosphoSitePlus, 2014: mutations, PTMs and recalibrations. *Nucleic Acids Research* **43**, D512–D520 (2015).

31. Marzoll, D. *et al.* Casein kinase 1 and disordered clock proteins form functionally equivalent, phospho-based circadian modules in fungi and mammals. *Proc. Natl. Acad. Sci. U.S.A.* **119**, e2118286119 (2022).
32. Vielhaber, E., Eide, E., Rivers, A., Gao, Z.-H. & Virshup, D. M. Nuclear Entry of the Circadian Regulator mPER1 Is Controlled by Mammalian Casein Kinase I ε. *Mol Cell Biol* **20**, 4888–4899 (2000).
33. Schittek, B. & Sinnberg, T. Biological functions of casein kinase 1 isoforms and putative roles in tumorigenesis. *Mol Cancer* **13**, 231 (2014).
34. Cruciat, C.-M. Casein kinase 1 and Wnt/β-catenin signaling. *Current Opinion in Cell Biology* **31**, 46–55 (2014).
35. Öllinger, R. *et al.* Dynamics of the circadian clock protein PERIOD2 in living cells. *Journal of Cell Science* jcs.156612 (2014) doi:10.1242/jcs.156612.
36. Smyllie, N. J. *et al.* Visualizing and Quantifying Intracellular Behavior and Abundance of the Core Circadian Clock Protein PERIOD2. *Current Biology* **26**, 1880–1886 (2016).
37. Smyllie, N. J. *et al.* Cryptochrome proteins regulate the circadian intracellular behavior and localization of PER2 in mouse suprachiasmatic nucleus neurons. *Proc. Natl. Acad. Sci. U.S.A.* **119**, e2113845119 (2022).
38. Xie, P. *et al.* Mammalian circadian clock proteins form dynamic interacting microbodies distinct from phase separation. *Proc. Natl. Acad. Sci. U.S.A.* **120**, e2318274120 (2023).
39. Hennig, S. *et al.* Structural and Functional Analyses of PAS Domain Interactions of the Clock Proteins Drosophila PERIOD and Mouse PERIOD2. *PLoS Biol* **7**, e1000094 (2009).

40. Sillibourne, J. E., Milne, D. M., Takahashi, M., Ono, Y. & Meek, D. W. Centrosomal Anchoring of the Protein Kinase CK1δ Mediated by Attachment to the Large, Coiled-coil Scaffolding Protein CG-NAP/AKAP450. *Journal of Molecular Biology* **322**, 785–797 (2002).
41. Cao, X., Wang, L., Selby, C. P., Lindsey-Boltz, L. A. & Sancar, A. Analysis of mammalian circadian clock protein complexes over a circadian cycle. *Journal of Biological Chemistry* **299**, 102929 (2023).
42. Badura, L. *et al.* An Inhibitor of Casein Kinase Iϵ Induces Phase Delays in Circadian Rhythms under Free-Running and Entrained Conditions. *J Pharmacol Exp Ther* **322**, 730–738 (2007).
43. Penas, C. *et al.* Casein Kinase 1δ Is an APC/CCdh1 Substrate that Regulates Cerebellar Granule Cell Neurogenesis. *Cell Reports* **11**, 249–260 (2015).
44. Graves, P. R. & Roach, P. J. Role of COOH-terminal Phosphorylation in the Regulation of Casein Kinase Iδ. *Journal of Biological Chemistry* **270**, 21689–21694 (1995).
45. Okamura, H. *et al.* A Conserved Docking Motif for CK1 Binding Controls the Nuclear Localization of NFAT1. *Mol Cell Biol* **24**, 4184–4195 (2004).
46. Xing, W. *et al.* SCFFBXL3 ubiquitin ligase targets cryptochromes at their cofactor pocket. *Nature* **496**, 64–68 (2013).
47. Nangle, S. N. *et al.* Molecular assembly of the period-cryptochrome circadian transcriptional repressor complex. *eLife* **3**, e03674 (2014).
48. Greer, Y. E. *et al.* Casein kinase 1δ functions at the centrosome and Golgi to promote ciliogenesis. *MBoC* **25**, 1629–1640 (2014).

49. Elmore, Z. C., Guillen, R. X. & Gould, K. L. The kinase domain of CK1 enzymes contains the localization cue essential for compartmentalized signaling at the spindle pole. *MBoC* **29**, 1664–1674 (2018).
50. Milne, D. M., Looby, P. & Meek, D. W. Catalytic Activity of Protein Kinase CK1δ (Casein Kinase 1δ) Is Essential for Its Normal Subcellular Localization. *Experimental Cell Research* **263**, 43–54 (2001).
51. Lowrey, P. L. *et al.* Positional Syntenic Cloning and Functional Characterization of the Mammalian Circadian Mutation *tau*. *Science* **288**, 483–491 (2000).
52. Meng, Q.-J. *et al.* Setting Clock Speed in Mammals: The CK1ε tau Mutation in Mice Accelerates Circadian Pacemakers by Selectively Destabilizing PERIOD Proteins. *Neuron* **58**, 78–88 (2008).
53. Fung, H. Y. J., Fu, S.-C., Brautigam, C. A. & Chook, Y. M. Structural determinants of nuclear export signal orientation in binding to exportin CRM1. *eLife* **4**, e10034 (2015).
54. Cunha, B. A., Sibley, C. M. & Ristuccia, A. M. Doxycycline: *Therapeutic Drug Monitoring* **4**, 115 (1982).
55. Lu, J. *et al.* Types of nuclear localization signals and mechanisms of protein import into the nucleus. *Cell Commun Signal* **19**, 60 (2021).
56. Gabriel, C. H. *et al.* Live-cell imaging of circadian clock protein dynamics in CRISPR-generated knock-in cells. *Nat Commun* **12**, 3796 (2021).
57. Narumi, R. *et al.* Mass spectrometry-based absolute quantification reveals rhythmic variation of mouse circadian clock proteins. *Proc. Natl. Acad. Sci. U.S.A.* **113**, (2016).

58. Park, J., Lee, K., Kim, H., Shin, H. & Lee, C. Endogenous circadian reporters reveal functional differences of *PERIOD* paralogs and the significance of PERIOD:CK1 stable interaction. *Proc. Natl. Acad. Sci. U.S.A.* **120**, e2212255120 (2023).
59. Rey, G. *et al.* Genome-Wide and Phase-Specific DNA-Binding Rhythms of BMAL1 Control Circadian Output Functions in Mouse Liver. *PLoS Biol* **9**, e1000595 (2011).
60. Hoffmann, J. *et al.* Non-Circadian Expression Masking Clock-Driven Weak Transcription Rhythms in U2OS Cells. *PLoS ONE* **9**, e102238 (2014).
61. Brown, S. A. *et al.* Molecular insights into human daily behavior. *Proc. Natl. Acad. Sci. U.S.A.* **105**, 1602–1607 (2008).

Figure Legends

Fig 1. Subcellular dynamics of overexpressed PER2 and CRY1

(A) Transient transfection of U2OStx cells and DOX-induced expression PER2-mNG (green) and mK2-CRY1 (magenta) results in nuclear foci. Scale bar 25 µm.

(B) Line plot analysis of inset of (A) shows co-localization of PER2-mNG and mK2-CRY1 in nuclear foci.

(C) CRY1 and PER2 mutually affect their subcellular localization. DOX-induced transiently expressed mK2-CRY1 (top row) and PER2-mNG (bottom row) individually and in combination was analyzed over 28 h. Co-expression was assessed at mK2-CRY1 : PER2-mNG ratios of 3:1 (second row), 1:1 (third row), and 1:3 (fourth row). Scale bar 25 µm.

(D) PER2-mNG exhibits rapid nucleo-cytoplasmic shuttling with a preference for the cytoplasm at early timepoints. DOX-induced expression of PER2-mNG in absence (DMSO) and presence of leptomycin B (LMB). Scale bar 25 mm.

(E) Expression of PER2-mNG supports accumulation of endogenous CRY1. Western blot analysis of U2OStx cells transiently transfected and DOX-induced with PER2-mNG sampled at various time points post-DOX induction. (The transfection efficiency of U2OStx cells is low.)

Fig 2. PERs and CRYs in nuclear foci retain their interaction specificity

(A) Schematic of experimental setup: U2OStx_mK2-CRY1 cells were transfected with PER2 and DOX-induced. Cells were analyzed for mK2-CRY1 expression and by immunofluorescence with antibodies against PER2 (B), PER1 (C), BMAL1 (D), and CK1δ (E).

(B) mK2-CRY1 and PER2 accumulate in nuclear foci. Scale bar 10 µm.

(C) Nuclear mK2-CRY1:PER2 foci contain endogenous PER1. Scale bar 10 µm.

(D) Nuclear foci contain endogenous BMAL1. Scale bar 10 µm.

(E) Nuclear foci contain endogenous CK1δ. Scale bar 10 µm.

Fig 3. CK1δ is stability regulated in an activity-dependent manner

(A) qPCR analysis of *CK1δ* mRNA in U2OStx cells and stable U2OStx cell lines expressing DOX-inducible CK1δ1, CK1δ1-K38R, and CK1δ1-R178Q. n = 3, Students t-test, ns: not significant.

(B) Immunoblot analysis of DOX-induced CK1δ variants. Upper panel: DOX-induced expression of indicated FLAG-tagged CK1δ1 variants in stable U2OStx cell lines. Lower panel: Expression of endogenous CK1δ (open circle) and CK1δ1-FLAG variants (filled circle) analyzed with antibody detecting endogenous and transgenic CK1δ.

(C) Overexpressed CK1δ1 is unstable with a half-life of about 6 min. CK1δ1-K38R and CK1δ1-R178Q are stable over 90 min. U2OStx_CK1δ1 cells were DOX-treated for 24 h and then treated with CHX. Samples were collected after the indicated time periods (CHX chase) and analyzed by immunoblotting with FLAG antibody.

(D) Endogenous CK1δ is stable over 90 min post CHX chase.

(E) Quantification of (C) and (D). n = 3, solid and dashed lines: mean ± SD.

(F) Left panel: Inhibition by PF670 stabilizes overexpressed FLAG-tagged CK1δ1. Right panel: 1h PF670 treatment of control cells has no effect on endogenous CK1δ levels. More protein (4x) was loaded on the gel for the analysis of endogenous CK1δ.

(G) Proteasomal inhibition by MG132 (4 h) stabilizes overexpressed (left panel) CK1δ1 and, (middle panel) to a lesser extent, the already stable CK1δ1-K38R. Right panel: MG132 has no effect on endogenous CK1δ levels in U2OStx control cells within the 4 h treatment window.

Fig 4. PER2 supports accumulation of endogenous CK1δ

(A) Endogenous CK1δ co-accumulates with overexpressed V5-PER2. Stable U2OStx_V5-PER2 cells were DOX-induced and analyzed after the indicated time periods for expression of (upper panel) V5-PER2 and (lower panel) endogenous CK1δ.

(B) Overexpressed CK1δ1 is stabilized dependent on PER2 dosage and PER-CK1δ interaction. HEK293T co-expression of CK1δ1-FLAG (200 ng) with increasing V5-PER2 results in V5-PER2 dose-dependent stabilization of CK1δ1-FLAG. Coexpression with V5-PER2ΔCKBD does not substantially stabilize CK1δ1-FLAG. All samples are from the same gel and Western blot, dashed vertical lines indicate that gel lanes with lower PER2 levels and size marker lanes were spliced out.

(C) PER2 stabilizes CRY1 and CK1δ1. HEK293T cell expression of indicated combinations of V5-PER2, mK2-CRY1, and CK1δ1-FLAG.

Fig 5. Active kinase is primarily degraded in the nucleus

(A) Endogenous CK1δ exhibits diffuse cellular localization with one distinct spot likely corresponding to the centrosome[48]. U2OStx was stained with DAPI (blue) and an antibody against CK1δ (green; AF488). Scale bar 20 µm.

(B) Immunofluorescene of U2OStx cell lines overexpressing FLAG-tagged CK1δ1, CK1δ1-K38R and CK1δ1-R178Q. Cells were DOX-treated for 24 h and stained via FLAG antibody (green; AF488) and with DAPI (blue). Scale bar 20 µm.

(C) Proteasomal inhibition by MG132 results in accumulation of overexpressed CK1δ1 primarily in nucleus. Stable U2OStx_CK1δ1 cells were DOX-induced for 24 h and treated with 5 µM MG132 for 4 h. Left: IF. Right: Quantification of CK1δ1 levels in MG132-treated cells versus vehicle (DMSO) control. $n \geq 50$ cells; mean ± SD; ****: $p < 0.0001$. Scale bar 20 µm.

(D) Kinase inhibition results in accumulation of overexpressed FLAG-tagged CK1δ specifically in the nucleus. Stable U2OStx_CK1δ cells were DOX induced for 24 h and treated with 1 µM PF670 for 1 h. Left: IF. Right: Quantification of CK1δ1 levels in PF670-treated cells versus vehicle (H_2O) control. $n \geq 50$ cells; mean ± SD; **: $p < 0.01$. Scale bar 20 µm.

(E) NES-tagged FLAG-CK1δ1-K38R accumulates at elevated levels in the cytoplasm and localizes to the centrosome. U2OStx cells were transiently transfected with either FLAG-CK1δ-K38R or NES-FLAG-CK1δ1-K38R. Left: FLAG-IF. Right: Quantification of kinase levels. $n \geq 20$ cells; mean ± SD; ****: $p < 0.0001$. Scale bar 20 µm.

Fig 6. CK1δ facilitates cytoplasmic accumulation of PER2 and release of CRY1

(A) Transient transfection and coexpression of PER2-mNG and mK2-CRY1 in U2OStx_CK1δ1 and U2OStx_CK1δ1-K38R stable cell lines. Expression was DOX-induced 24 h post transfection and cells were then analyzed for 24 h with an Incucyte system. PER2-mNG and mK2-CRY1 accumulate in nuclear foci when coexpressed with inactive CK1δ1-K38R (upper row) and in cytoplasmic foci when coexpressed with active CK1δ1 (lower row). Scale bar 20 µm.

(B) Cytoplasmic PER2-mNG foci (CK1δ1 cells) contain less mK2-CRY1 than nuclear foci (CK1δ1-K38R cells). Scale bar 20 µm. Right: Quantification of CRY1 : PER2 ratio in cytoplasmic and nuclear foci. n > 30 foci, mean ± SD; ****: $p < 0.0001$.

(C) PER2 phosphorylation attenuates interaction with CRY1. V5-PER2 and CRY1-FLAG were transiently expressed in HEK293T. Cell lysate was prepared and incubated with and without recombinant CK1δΔtail for 4 h. V5-PER was then immunoprecipitated with V5 beads. Lysate (Input) and an 8x equivalent of the IP were analyzed by Western-blot. FLAG-CRY1 co-immunoprecipitated with hypophosphorylated but not with hyperphosphorylated V5-PER2 (n=3).

(D) Cytoplasmic PER:CRY foci persistently release CRY1 into the nucleus in a CK1δ1-dependent fashion. Scale bar 20 µm.

Central cell: Representative U2OStx_mK2-CRY1 cell co-transfected with PER2-mNG and CK1δ1, resulting in the formation of cytoplasmic PER:CRY foci. Over time, PER2-mNG levels decrease, while mK2-CRY1 accumulates in the nucleus and remains at persistently high levels, even 36 hours post DOX induction (see Fig EV6 for more examples).

Surrounding cells: U2OStx_mK2-CRY1 cells not transfected with PER2-mNG. In these cells, mK2-CRY1 accumulates in the nucleus initially, but its levels decrease

over time, likely due to DOX metabolism, with low levels observed 36 hours post DOX induction.

Fig 7. Nuclear CK1δ affects circadian period length

(A) Schematic of mNG-NLS-CK1δ1 and mNG-NES-CK1δ1 constructs NLS: SV40[53]; NES: HIV-1[55].

(B) Left: mNG-NLS-CK1δ1 is expressed at a very low level in the nucleus and is stabilized by MG132. B/C-adjusted panel: brightness and contrast adjusted to better visualize the kinase. Right: quantification. n > 30 cells, mean ± SD; ****: $p < 0.0001$. Scale bar 20 µm.

(C) Left: mNG-NES-CK1δ localizes to the cytosol and is stabilized by MG132. Right: quantification. n > 30 cells, mean ± SD; ***: $p < 0.001$. Scale bar 20 µm.

(D) Stable U2OStx lines expressing comparable levels of DOX-induced FLAG-tagged mNG-NLS-CK1δ1 or mNG-NES-CK1δ1.

(E) DOX-induced expression of NLS-CK1δ1 results in significant period shortening whereas NES-CK1δ1 has no effect on period. *Bmal1* promoter-luciferase assay. Representative bioluminescence traces are shown as a detrended average of 4 technical replicates of PBS- and DOX-treated cells. Resulting period was calculated using cosinor analysis built-in GraphPad Prism 10.

(F) Circadian period change comparing DOX- vs. PBS-treated mNG-NLS-CK1δ1 or mNG-NES-CK1δ1 cell lines. n = 3, mean ± SD; **: $p < 0.01$.

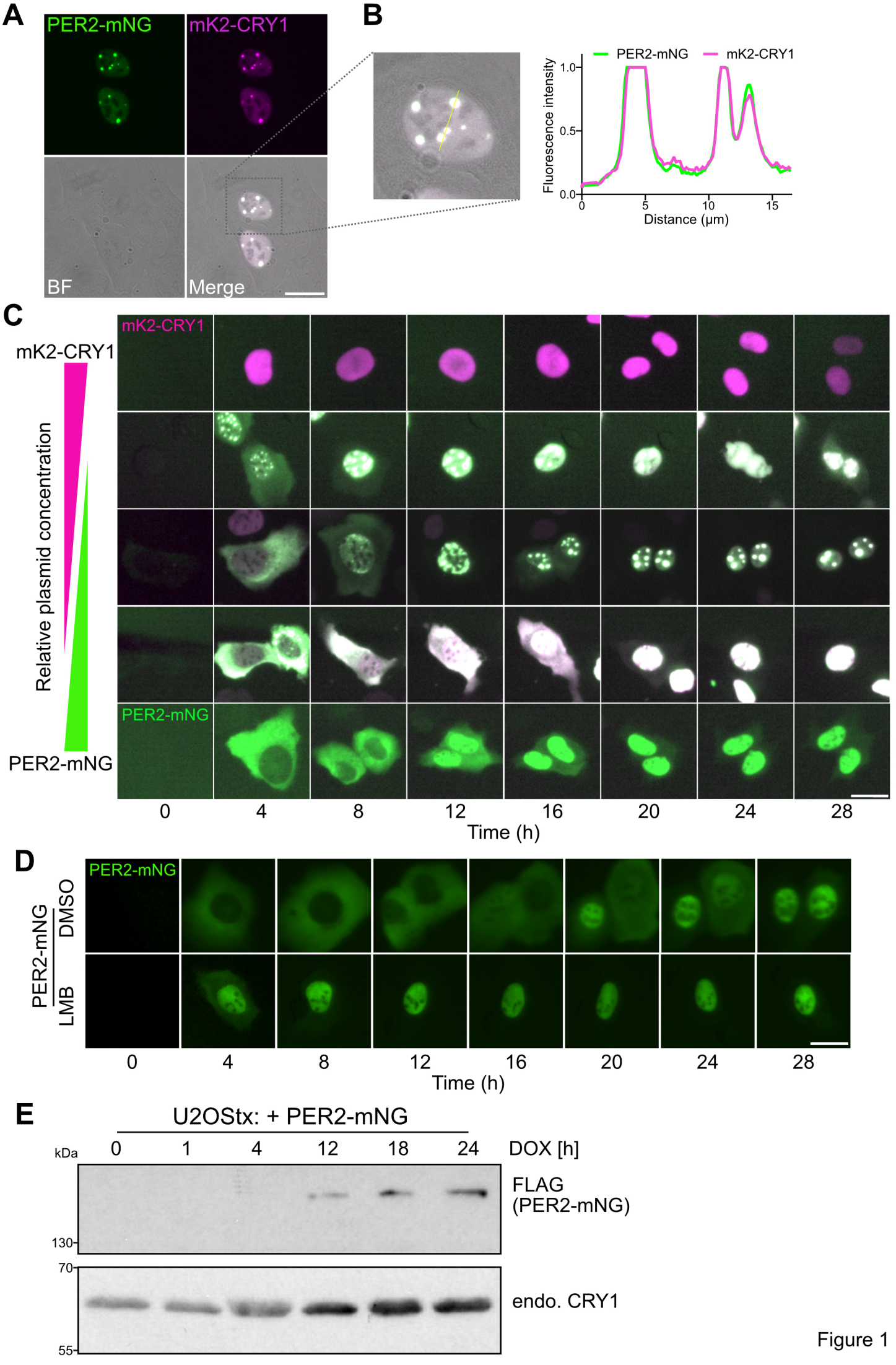
A
PER2-mNG
mK2-CRY1
BF
Merge
B
PER2-mNG
mK2-CRY1
Fluorescence intensity
1.0
0.5
0.0
0
5
10
15
Distance (µm)
C
mK2-CRY1
Relative plasmid concentration
PER2-mNG
0
4
8
12
16
20
24
28
Time (h)
D
PER2-mNG
PER2-mNG
DMSO
LMB
0
4
8
12
16
20
24
28
Time (h)
E
U2OStx: + PER2-mNG
kDa
0
1
4
12
18
24
DOX [h]
FLAG
(PER2-mNG)
130
70
endo. CRY1
55

Figure 1

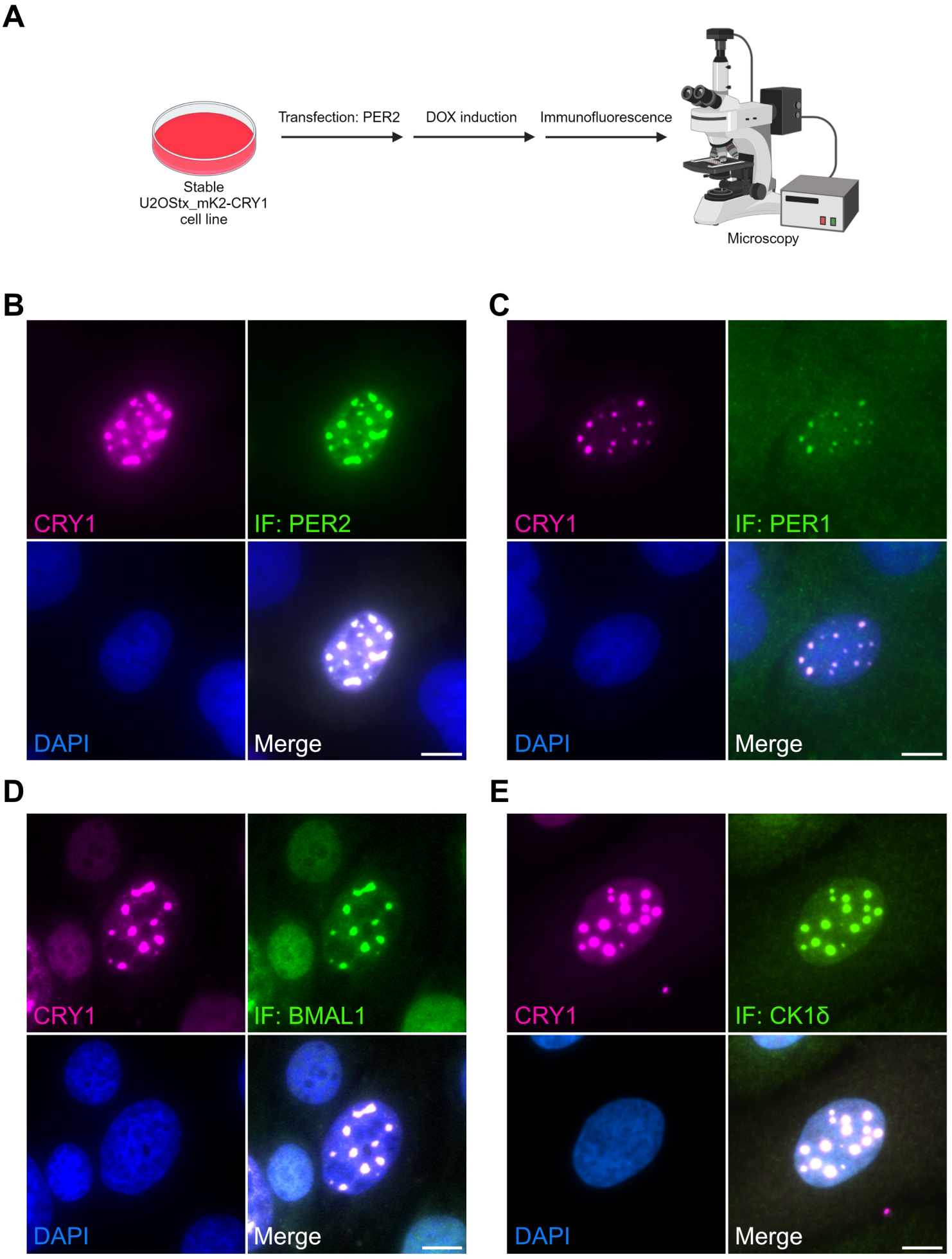
A
Stable
U2OStx_mK2-CRY1
cell line
Transfection: PER2
DOX induction
Immunofluorescence
Microscopy
B
CRY1
IF: PER2
DAPI
Merge
C
CRY1
IF: PER1
DAPI
Merge
D
CRY1
IF: BMAL1
DAPI
Merge
E
CRY1
IF: CK1δ
DAPI
Merge

Figure 2

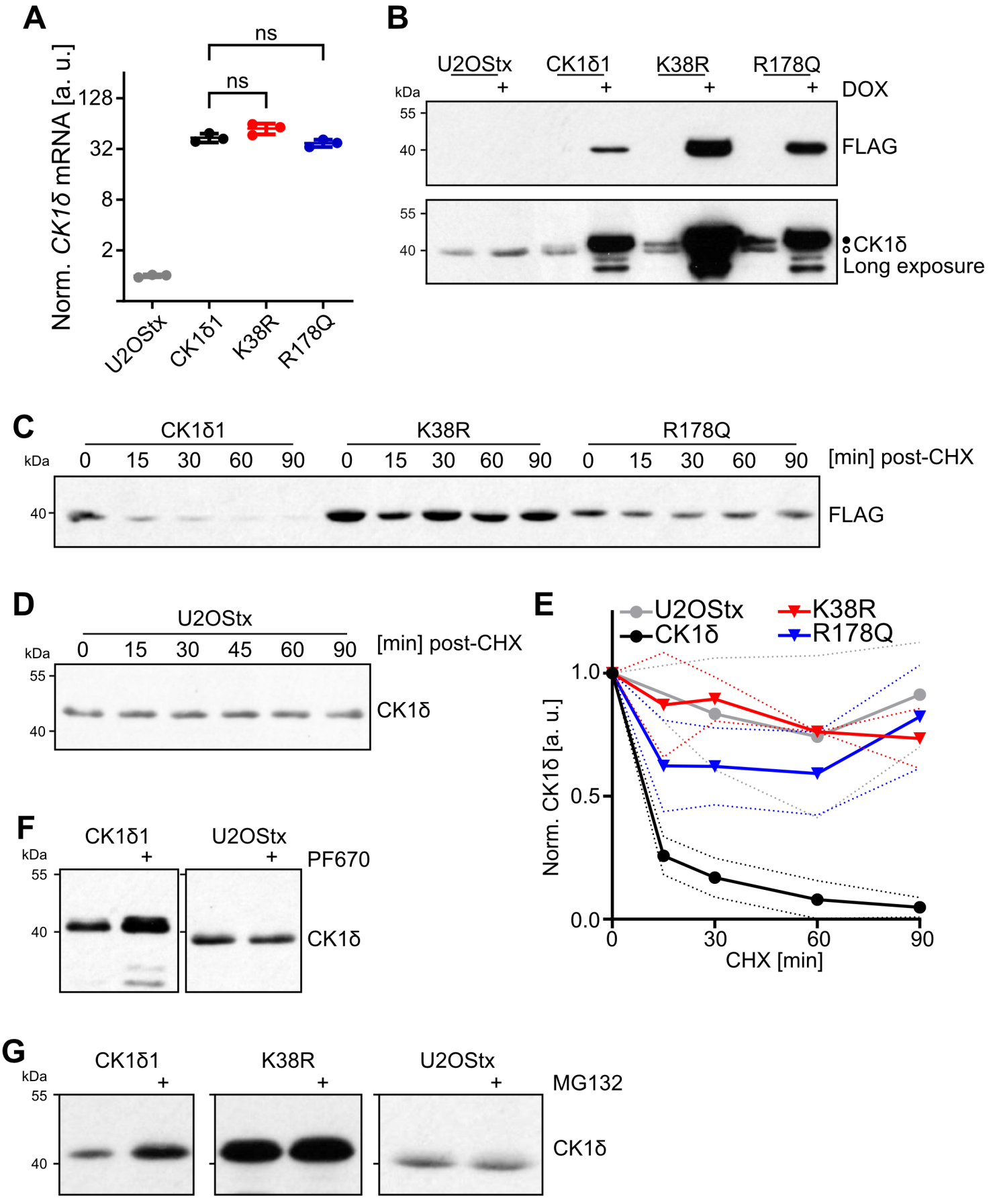
A
ns
ns
Norm. CK1δ mRNA [a. u.]
128
32
8
2
U2OStx
CK1δ1
K38R
R178Q
B
U2OStx
CK1δ1
K38R
R178Q
kDa
+
+
+
+
DOX
55
40
FLAG
55
40
CK1δ
Long exposure
C
CK1δ1
K38R
R178Q
kDa
0 15 30 60 90 0 15 30 60 90 0 15 30 60 90
[min] post-CHX
40
FLAG
D
U2OStx
kDa
0 15 30 45 60 90
[min] post-CHX
55
40
CK1δ
E
U2OStx
CK1δ
K38R
R178Q
Norm. CK1δ [a. u.]
1.0
0.5
0.0
0
30
60
90
CHX [min]
F
CK1δ1
U2OStx
kDa
+
+
PF670
55
40
CK1δ
G
CK1δ1
K38R
U2OStx
kDa
+
+
+
MG132
55
40
CK1δ

Figure 3

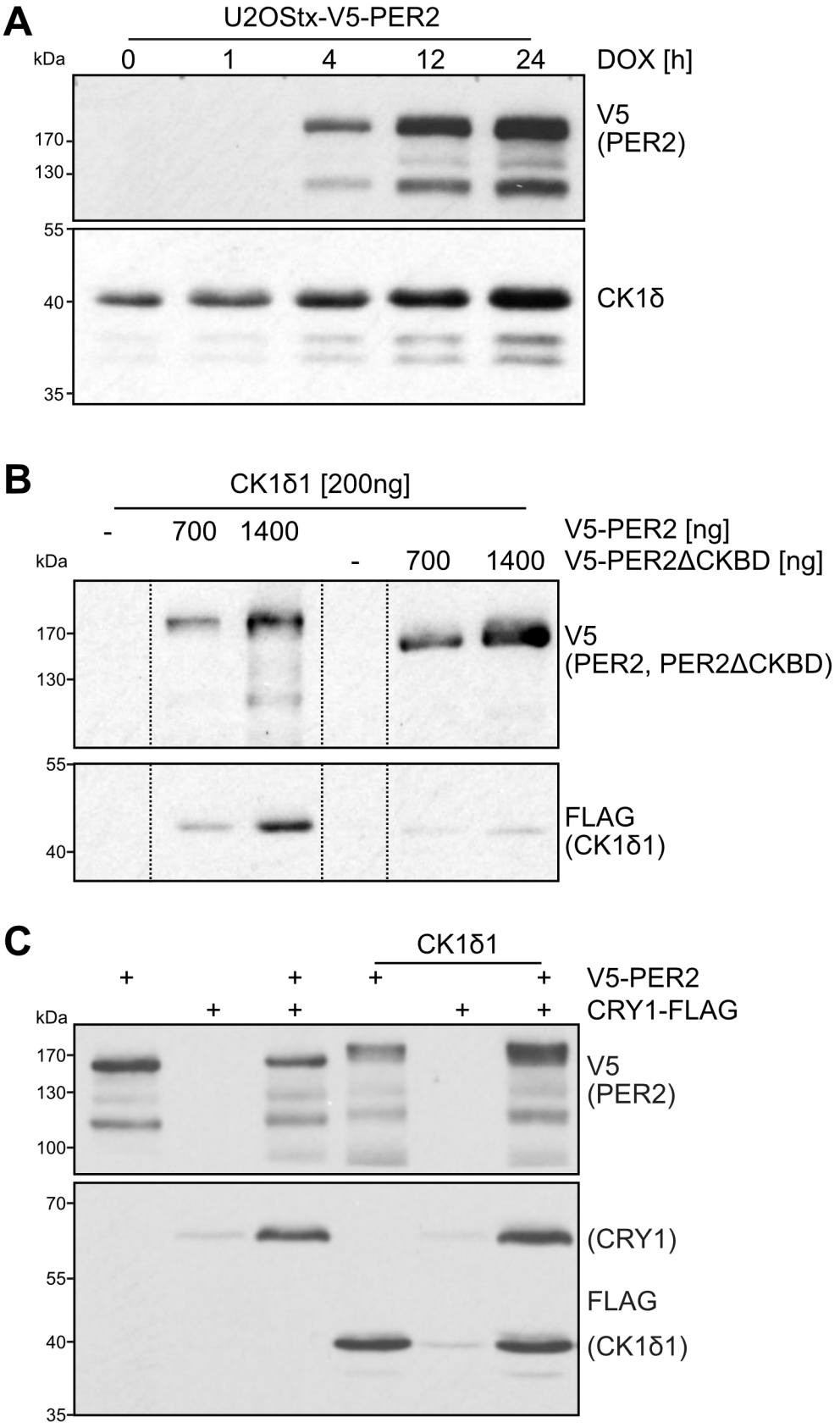
A
U2OStx-V5-PER2
kDa
0
1
4
12
24
DOX [h]
170
130
55
40
35
V5
(PER2)
CK1δ
B
CK1δ1 [200ng]
-
700
1400
V5-PER2 [ng]
-
700
1400
V5-PER2ΔCKBD [ng]
kDa
170
130
55
40
V5
(PER2, PER2ΔCKBD)
FLAG
(CK1δ1)
C
CK1δ1
+
+
+
+
V5-PER2
+
+
+
+
CRY1-FLAG
kDa
170
130
100
70
55
40
35
V5
(PER2)
(CRY1)
FLAG
(CK1δ1)

Figure 4

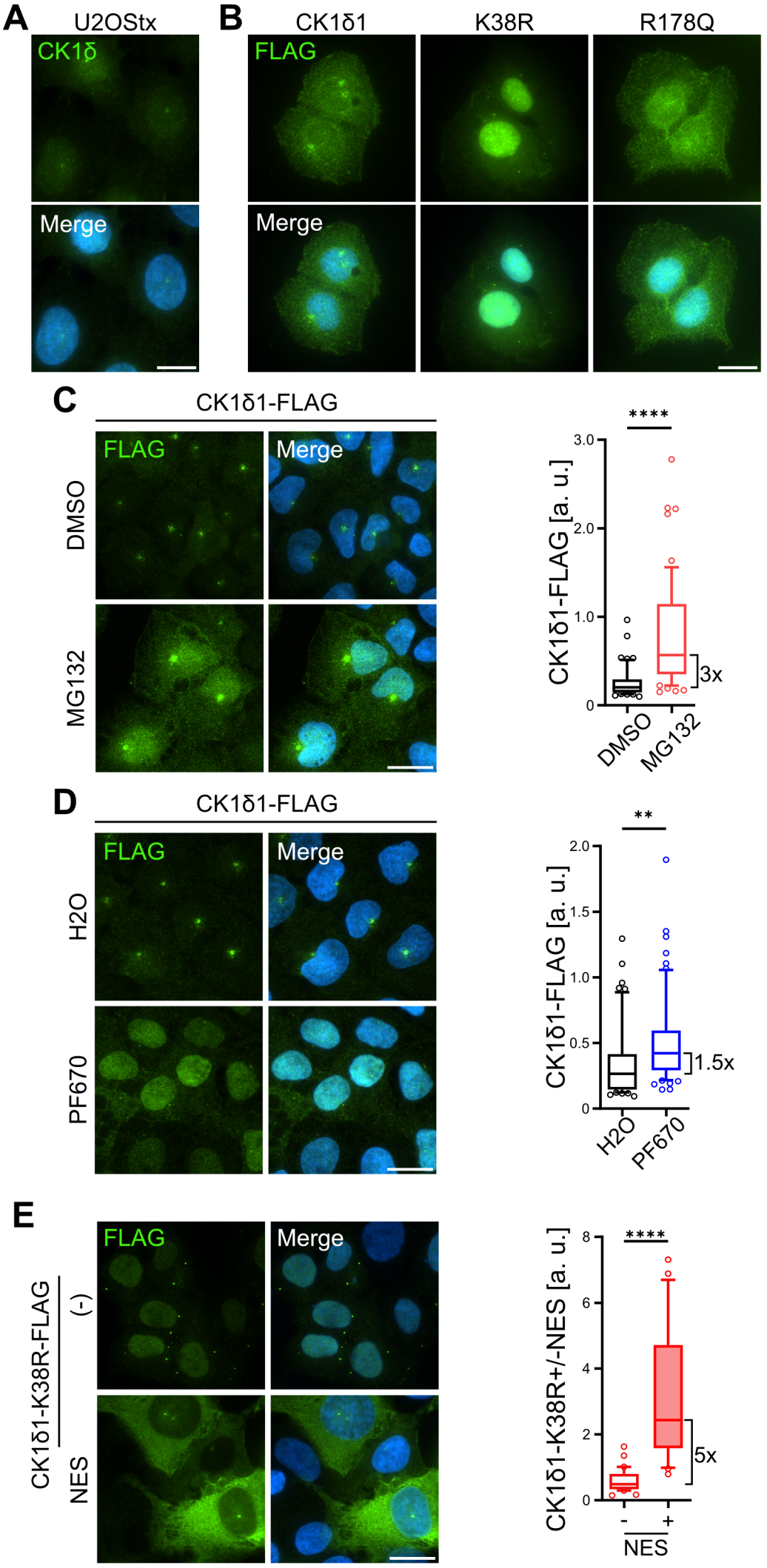
A
U2OStx
CK1δ
Merge
B
CK1δ1
K38R
R178Q
FLAG
Merge
C
CK1δ1-FLAG
DMSO
MG132
FLAG
Merge
****
CK1δ1-FLAG [a. u.]
3.0
2.0
1.0
0
3x
DMSO
MG132
D
CK1δ1-FLAG
H2O
PF670
FLAG
Merge
**
CK1δ1-FLAG [a. u.]
2.0
1.5
1.0
0.5
0
1.5x
H2O
PF670
E
CK1δ1-K38R-FLAG
(-)
NES
FLAG
Merge
****
CK1δ1-K38R+/-NES [a. u.]
8
6
4
2
0
5x
-
+
NES

Figure 5

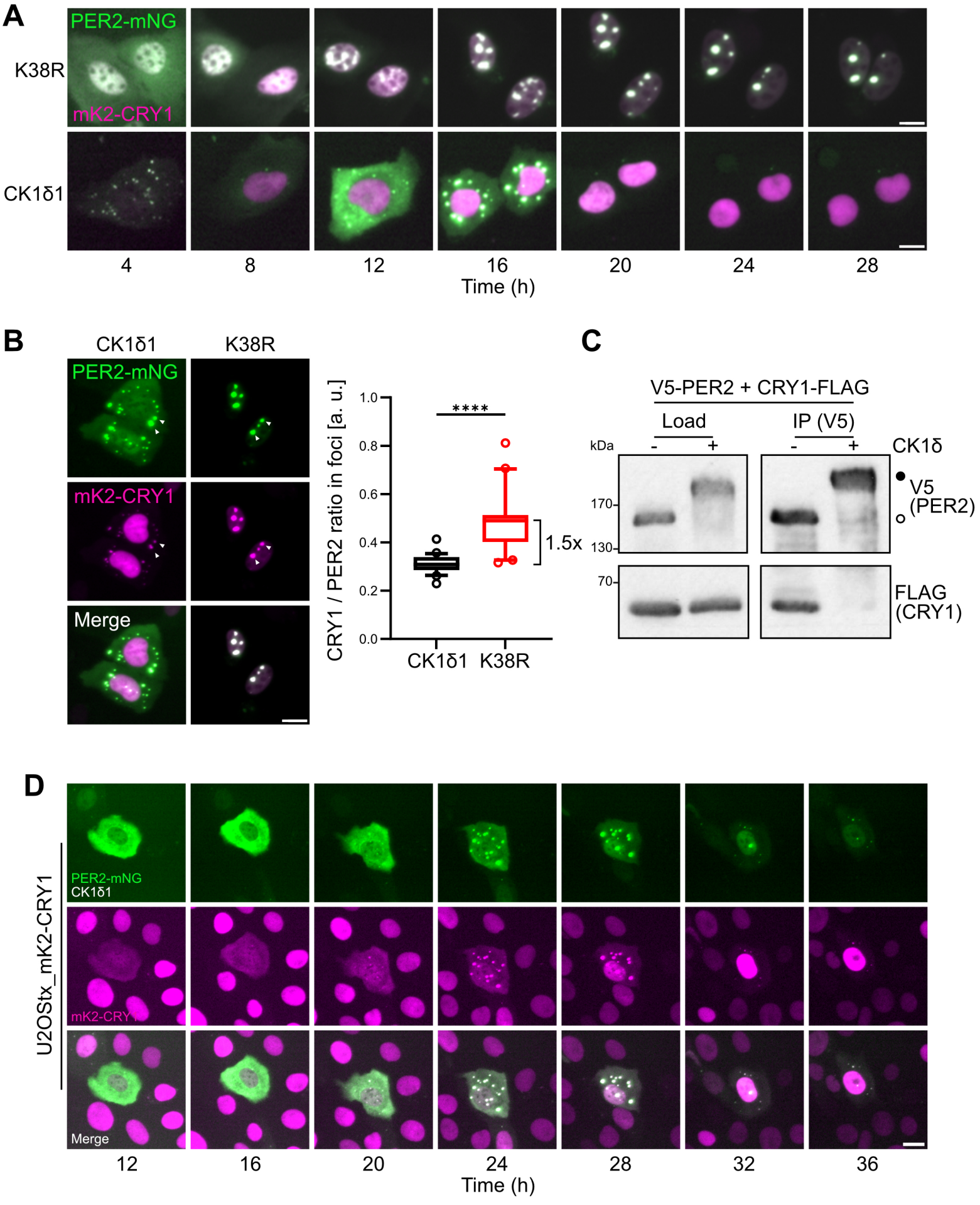
A
PER2-mNG
mK2-CRY1
K38R
CK1δ1
4
8
12
16
20
24
28
Time (h)
B
CK1δ1
K38R
PER2-mNG
mK2-CRY1
Merge
CRY1 / PER2 ratio in foci [a. u.]
1.0
0.8
0.6
0.4
0.2
0.0
****
1.5x
CK1δ1
K38R
C
V5-PER2 + CRY1-FLAG
Load
IP (V5)
kDa
-
+
-
+
CK1δ
170
130
70
V5
(PER2)
FLAG
(CRY1)
D
U2OStx_mK2-CRY1
PER2-mNG
CK1δ1
mK2-CRY1
Merge
12
16
20
24
28
32
36
Time (h)

Figure 6

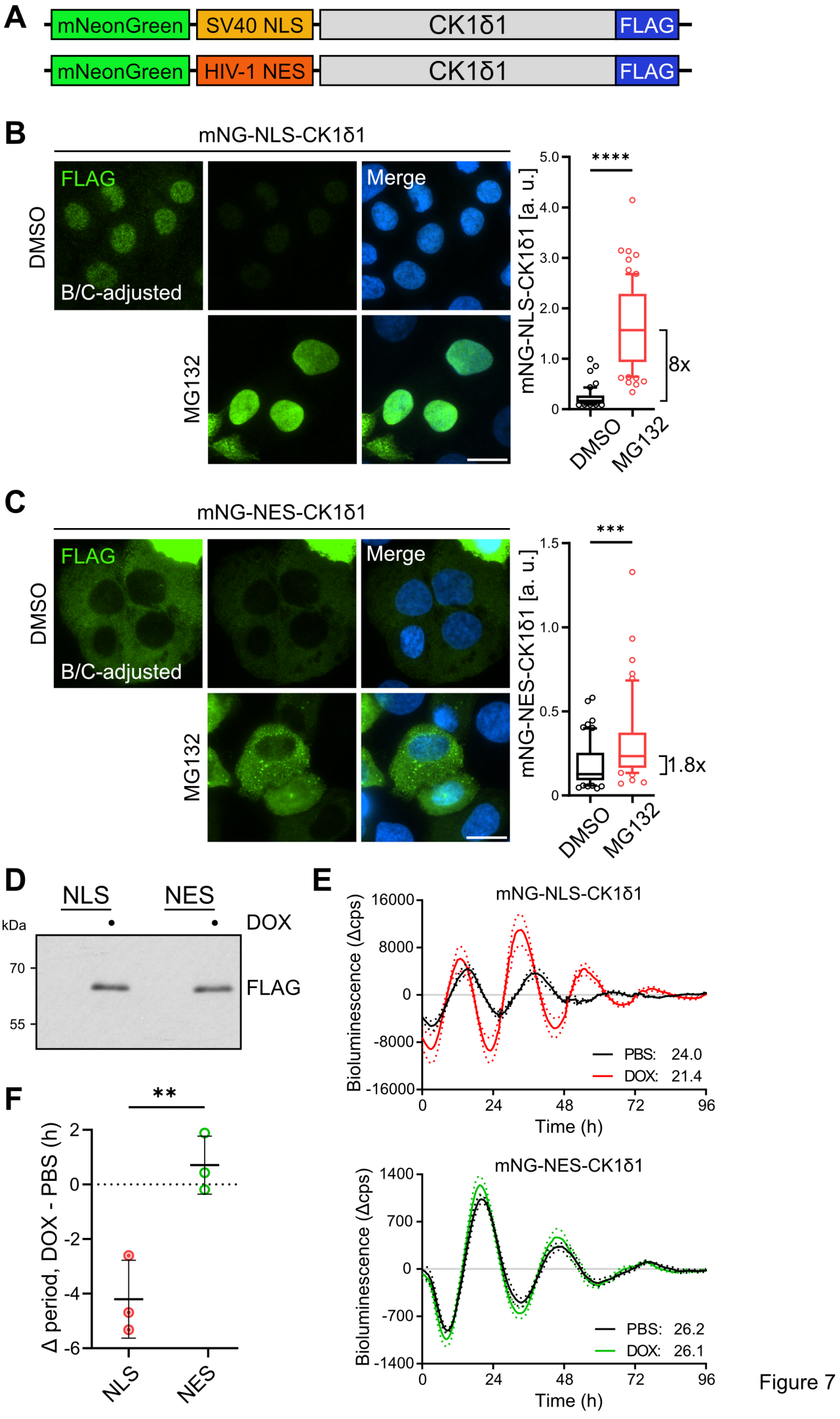
A
mNeonGreen
SV40 NLS
CK1δ1
FLAG
mNeonGreen
HIV-1 NES
CK1δ1
FLAG
B
mNG-NLS-CK1δ1
FLAG
Merge
DMSO
B/C-adjusted
MG132
mNG-NLS-CK1δ1 [a. u.]
****
8x
DMSO
MG132
C
mNG-NES-CK1δ1
FLAG
Merge
DMSO
B/C-adjusted
MG132
mNG-NES-CK1δ1 [a. u.]
***
1.8x
DMSO
MG132
D
NLS
NES
kDa
DOX
70
55
FLAG
E
mNG-NLS-CK1δ1
Bioluminescence (Δcps)
PBS: 24.0
DOX: 21.4
Time (h)
mNG-NES-CK1δ1
Bioluminescence (Δcps)
PBS: 26.2
DOX: 26.1
Time (h)
F
**
Δ period, DOX - PBS (h)
NLS
NES

Figure 7